American Mineralogist, Volume 67, pages 568–586, 1982

Crystal chemistry of clinopyroxenes from the St. Marcel manganese deposit, Val d'Aosta, Italy

WILLIAM L. GRIFFIN

Mineralogisk-Geologisk Museum
N-Oslo 5, Norway

AND ANNIBALE MOTTANA

Istituto di Mineralogia, Università
Città Universitaria, I-00185 Roma, Italy

Abstract

The St. Marcel manganese deposit, Val d'Aosta, Italy, lies within the ophiolite sequence of the Zermatt-Saas unit of the Piemonte nappe, and formed as a hydrothermal sediment at an oceanic spreading center. Eoalpine metamorphism to eclogite facies was followed by retrogression to lawsonite–glaucophane facies and Lepontine greenschist facies assemblages. The Mn-rich rocks contain a wide variety of clinopyroxenes in the Di–Jd–Ac plane. Massive pyroxene-rich rocks (±albite ±quartz) contain aegirine-jadeite and impure jadeite, zoned via chloromelanite to omphacite. Violet pyroxenes ("violan") in veins and in massive braunite ore are diopside, omphacite or chloromelanite. Di-Ac pyroxenes are breakdown products of omphacite/chloromelanite, or form late veins. Manganacmite substitution reaches 13% in some violans. X-ray data on 18 samples show that *C*2/*c* structures extend along the Di–Ac and Di–Jd joins to at least Ac_{60}; omphacites and an intermediate chloromelanite are of *P* type. Textural relations suggest that the various pyroxene compositions within each sample formed sequentially (zoning and/or replacement) through local changes in bulk composition, and should not be used to define solvi. The spread of *all* data points for 25 samples is consistent with a solvus between Jd_{60} and Jd_{85} on the Di–Jd join, but this gap closes at Ac > 20%.

Introduction

The composition of metamorphic clinopyroxenes can vary widely with variations in P, T, f_{O_2} and the chemistry of their host rocks. These compositional variations are a potentially powerful tool in petrogenetic studies, but many aspects of the crystal chemistry of these pyroxenes are still poorly understood. The Di–Ac–Jd system is of particular interest to studies of deep-crustal and upper mantle rocks, because it contains pyroxenes stable over a wide range of pressures and temperatures. However, the pressure–temperature range characteristic of blueschist facies metamorphism is mostly inaccessible to experimental studies because of kinetic problems at low T. Pyroxenes from blueschist-facies rocks have therefore been extensively studies for evidence of coexisting phases, exsolution or other relations that can illuminate their stability relations in natural systems. The results of these studies are in part contradictory.

The St. Marcel (Praborna) Mn-deposit in the Val d'Aosta, Italy, offers a unique opportunity to study a wide range of unusual bulk compositions metamorphosed at low T and high P. Many of these Mn-rich rocks are pyroxene-bearing, and omphacite, diopside and jadeite–acmite pyroxenes are common. This paper presents detailed textural, chemical and structural data on pyroxenes from 25 samples, covering much of the Di–Ac–Jd compositional plane and a variety of parageneses.

The St. Marcel deposit was extensively studied by mineralogists during the last century; manganiferous varieties of several common minerals have been described and named from this locality (piemontite; "alurgite", a manganoan phengite; "greenovite", a pink sphene). "Violan", the characteristic purple-blue clinopyroxene of St. Marcel, was first described by Breithaupt (1838) and reexamined by Des Cloizeaux (1862–1874) and Schluttig (1888). The early analyses are unsatisfac-

003–004X/82/0506–0568$02.00

tory, probably due to impurities, and the species was discredited by Penfield (1893) as "a blue variety of diopside, containing small quantities of well-known pyroxene molecules". However, Penfield himself noted the presence of other pyroxenes at St. Marcel, and presented an analysis of a greyish pyroxene with the composition of a chloromelanite. We will use the name "violan" here only to denote pyroxenes with a purple color.

Aside from a morphological description (Rondolino, 1934), no further studies on "violan" appeared until work was resumed by Mottana *et al.* (1977, 1979). Bondi *et al.* (1978) described pyroxenes from 20 samples, including the brown variety "schefferite" (Di–Ac solid solution) and Brown *et al.* (1978) gave detailed microprobe data on three samples. The present work was started in 1977 with the aim of unraveling the complex phase petrology, geochemistry and metamorphic history of the deposit. This will require an understanding of the complex crystal chemistry of several mineral groups. A study of the titanites (greenovites) has been published (Mottana and Griffin, 1979); this paper reports on the pyroxenes, and a study of the piemontites will follow (Mottana and Griffin, in prep.) Comparison of the phase petrology of this deposit with that of similar, but lower grade ones elsewhere in the Alps may ultimately allow a better understanding of low-*T*, high-*P* metamorphic processes in general.

Geological setting

The Praborna ore body is the largest manganese deposit of the western Alps (Burckardt and Falini, 1956). The deposit is one of many occurring within the Piemonte Ophiolite Nappe (see Huttenlocher, 1934; Debenedetti, 1965; Dal Piaz, 1971; Brigo *et al.*, 1976 for a systematic overview), more specifically in the upper unit of this nappe, known as the Zermatt-Saas unit (Bearth, 1967, 1976; Elter, 1971; Kienast, 1973; Dal Piaz, 1974a, b; Dal Piaz and Ernst, 1978). This unit, consisting mainly of metabasites with interbedded metasediments and slices of metaplutonic rocks, is believed to represent the oceanic crust of the Pennidic trough that was subducted and metamorphosed during the compressional stages of the alpine orogenesis.

In the St. Marcel Valley the Zermatt–Saas unit consists largely of metapelites with interbedded metamorphosed limestones, marls (calcschists) and quartzites, and of a metavolcanic sequence that includes serpentinized peridotites and metamorphosed gabbros, pillow lavas and tuffs. The rock types range from massive eclogites and glaucophanites (Franchi, 1900) to albite–chlorite–actinolite schists and felses (prasinites, ovardites) that often carry abundant sulphides. Three kilometers downstream from Praborna, the pyrite mines of Servette and Chuk, both occurring within metabasites, produced copper until a few years ago (Dal Piaz, 1971; Brigo *et al.*, 1976).

The manganese ore body lies stratigraphically just above the pyrite deposits (Huttenlocher, 1934) and overlies a sequence of massive "prasinites" containing garnet, glaucophane, large lawsonite porphyroblasts partially altered to muscovite, and disseminated pyrite. The ore body is overlain by another sequence of schistose chlorite–actinolite–sericite–albite metabasites that are rich in albite–hematite veins and locally grade into metagabbros with fuchsite and actinolite. These rocks in turn underlie a wedge of calcschists and antigorite schists.

The ore body itself (Priesshäusser, 1980; Pelloux, 1922; Huttenlocher, 1934) is a complexly folded layer of banded quartzites, the thickness of which varies between 0.4 and 4 m, reaching a maximum of 9 m in a large fold nose at the mine opening. The banded structure of the quartzite is particularly well exposed toward the top of the deposit, where a clearly defined, 50-150 cm thick marker layer consists of reddish piemontite quartzite enclosing bright yellow pods of quartz + spessartine ± rhodonite/pyroxmangite. This marker horizon shows tight isoclinal folds, refolded by more gentle folds on a scale of meters. It can be followed laterally for *ca.* 60 m before pinching out in a series of pods and lenses made conspicuous by their reddish or yellowish color or by the presence of braunite knobs. The pods are brecciated and cemented by quartz and rhodonite. This horizon locally grades downward to phengite–piemontite–carbonate–quartz ± clinopyroxene schists.

The main ore body consists largely of braunite + quartz in cm-thick bands, but locally is rather massive. Pyroxenites ± manganoan phengite ("alurgite") form boudined layers up to 10 cm thick within the braunite.

The ore body is crossed by several types of veins so that it is locally a breccia, particularly toward the lower and upper margins. The most common vein minerals are "alurgite", in rather large pink flakes, piemontite in crystals up to several cm in length, albite, titanite, and several varieties of clinopyrox-

Table 1. Replicate EDS analyses of $Di_{65}Jd_{35}$ glass

	1979 (24 anal.)	1980 (24 anal.)	σ_{n-1}	Given comp.
SiO_2	56.72	56.67	0.44	56.88
TiO_2	0.0	0.0	-	0.0
Al_2O_3	9.10	9.00	0.17	8.82
FeO	0.07	0.07	0.09	0.0
MnO	0.0	0.0	-	0.0
MgO	12.11	12.06	0.19	12.10
CaO	16.95	17.02	0.18	16.83
Na_2O	5.26	5.28	0.14	5.37
Σ	100.21	100.10		100.00
Jd	35.9	36.0		36.6
Di	63.3	63.4		63.4

ene. The last veins to form consist of a whitish fibrous tremolite that coats the smallest cracks.

The lower contact of the ore body is a thin (1–10 cm) but continuous reddish layer mainly composed of piemontite, albite, and quartz. This is underlain successively by a massive spessartine–piemontite–quartz fels and by a strongly foliated phengite–piemontite–carbonate quartzite with local, minor braunite and pyroxene. The contact to the underlying metabasites is rather sharp.

The Praborna ore body, like the manganiferous cherts occurring in eastern Liguria (Brigo *et al.*, 1976), may have formed at an oceanic spreading center (*cf.* Bonatti *et al.*, 1976). Our preliminary results show considerable anomalies in Ba and Sr, and the high Si/Al ratio of these cherts is typical of metalliferous sediments near mid-oceanic spreading centers. The relationship with cupriferous pyrite deposits, and the abundant pyrite in the underlying metabasites, may be related to circulation of high temperature hydrothermal fluids, causing precipitation of FeS_2 in basalts of the spreading center and leaching of Mn from the oceanic crust (Bonatti *et al.*, 1972a, b; Bonatti, 1975; Boström, 1976).

The metamorphic history of the Zermatt–Saas unit of the Piemonte Ophiolite Nappe (Dal Piaz, 1974a, b; Frey *et al.*, 1974; Fry and Fyfe, 1971) involved at least two stages. An Eoalpine high pressure–low temperature phase (dated to 80–90 m.y.: Delaloye and Desmons, 1976; Bocquet *et al.*, 1974) culminated with the formation of eclogites at 470±50°C and 10±2 kbar (Ernst and Dal Piaz, 1978). A low pressure phase, representing the buoyant return toward the surface, was related to the Lepontine phase of the central Alps (38 m.y.; Jaeger, 1973). The *P–T* conditions of the latter have been estimated for the lower Val d'Aosta to be in the vicinity of 400°C and 3 kbar, at fluid pressures approaching the total pressure (Ernst and Dal Piaz, 1978).

Analytical methods

Microprobe analyses were carried out at the Mineralogisk-Geologisk Museum, Oslo, using an ARL-EMX probe fitted with a LINK energy-dispersive analytical system. Spectrum deconvolution was done by multiple least-squares fitting and standard matrix correction procedures (program ZAF-4) were used. Standards included pure metals, synthetic oxides and natural minerals. Repeated analyses of mineral standards over the period covered by the analyses presented here show precision and accuracy comparable to wavelength-dispersive techniques for abundances over *ca.* 0.2–0.3% (see Table 1).

The unit-cell parameters were determined from handpicked powdered material using Si as the internal standard. Data were collected with a vertical diffractometer using a scan speed of 0.25° 2θ/min. The self-indexing least-squares program of Evans *et al.* (1963), modified to run on the UNIVAC 1100/20 computer of the University of Rome, was used for the computation. At least six reflections, easy to identify by comparison with the tables of Borg and Smith (1969), were kept constant throughout the cycles.

The lattice type was determined using a single-crystal diffractometer by monitoring *h0l* reflections with $h + l \neq 2n$, typical for the P-type lattice, relative to those with $h + l = 2n$ as in the C-type lattice (see Rossi *et al.*, 1978).

Occurrence and petrography of clinopyroxenes

For convenience, the samples studied here can be divided into several general types.

(1) The "typical violan" of St. Marcel occurs in coarse-grained veins and segregations. Pre- or syn-metamorphic albite ± quartz veins brecciate the braunite ore, especially in the roof of the ore body, and commonly contain the darkest-purple pyroxenes. Apparently post- or late-metamorphic veins of albite + quartz contain paler-colored pyroxenes, commonly associated with dark red piemontites. In both occurrences the subhedral pyroxene forms large (to 1 cm) bladed masses with subradial habits. The existence of abundant subgrain boundaries in

the pyroxenes, as well as other evidence of strain in both pyroxenes and other phases, indicate that the "lamellar" structure is due to deformation of originally larger grains. Euhedral "violan" occurs very rarely as small crystals in calcite-filled vugs within the ore (Mottana *et al.*, 1979).

Earlier studies of these bladed ("lamellar") pyroxenes by Mottana *et al.* (1977, 1979), Bondi *et al.* (1978), and Brown *et al.* (1978) showed that they are either diopsidic or omphacitic in composition, and that some specimens have discrete domains of diopside, impure diopside, and omphacite. The pyroxenes examined in all of these studies were so similar optically that the textural, and genetic, relations of the different compositions were obscure.

In our sample SM103, microprobe analysis reveals a very strong correlation of color with composition, which allows study of texture/composition relations in thin sections. Long prisms of both colorless diopside (Jd + Ac + MnAc $<$ 10%) and pale violan (Jd + Ac + MnAc $\geq$ 20%) grow across patches of relict tremolite, and project into a quartz vein. The diopside in turn is continuously zoned to pale violan at grain boundaries and along cracks. The blades of pale violan are continuously zoned to dark purple omphacite (Jd + Ac + MnAc up to 45%). Both diopside and pale violan are also bordered and transected by trains of granular dark omphacite grains. The textures strongly suggest that the rock initially consisted of tremolite + quartz (or tremolite + diopside + quartz?) and that the complex pyroxenes grew in response to metasomatic introduction of Na, Al, Fe and Mn.

(2) Fine- to medium-grained massive pyroxenites or clinopyroxene + piemontite ± phengite ("alurgite") rocks occur as layers and boudins within the ore body. The pyroxenes in these rocks commonly show several stages of development, from pale aegirine-jadeite cores to jadeite, chloromelanite, or omphacite rims. These major variations in composition are usually accompanied by color differences,

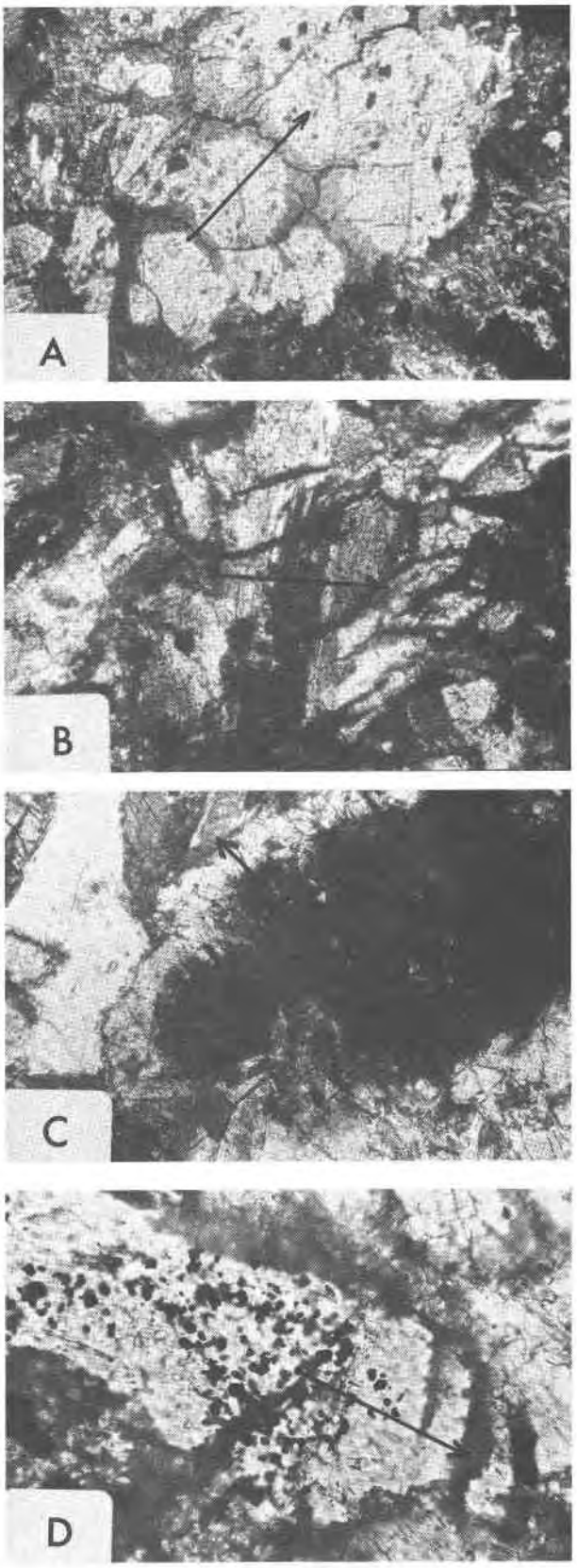

Fig. 1. Photomicrographs of St. Marcel pyroxenes. Arrows show location and direction (left to right) of analysis traverses in Figure 2. (a) SM89. Aegirine-jadeite grains (light) irregularly replaced along grain boundaries by jadeite (dark). Crossed nicols; (b) SM88. Irregular "lamellae" (cores) of aegirine-jadeite (dark) in jadeite (light). Crossed nicols; (c) SM102. Aegirine-jadeite core (dark) continuously zoned to rim of chloromelanite. Crossed nicols; (d) SM7. Core of aegirine-jadeite (with braunite inclusions) surrounded by successive rims of chloromelanite and omphacite.

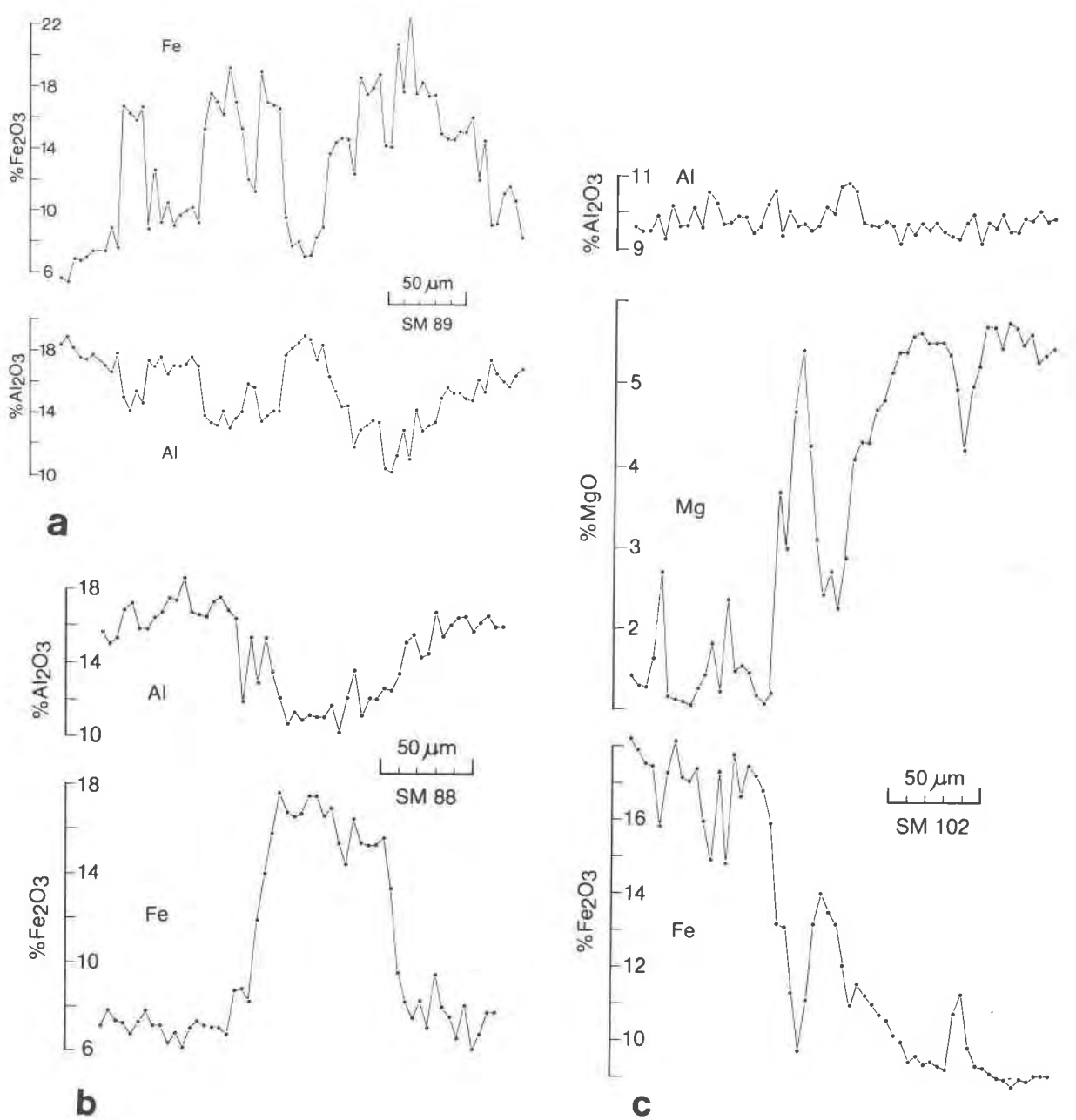

Fig. 2. Microprobe traverses across pyroxene grains shown in Figure 1.

so that their textural relations may be studied in detail using thick sections. Some examples are illustrated in Figures 1 and 2. Strain is generally less pronounced in these rocks than in the first type.

SM88 is a medium-grained pyroxenite with a mosaic texture (Fig. 1b). Each pyroxene grain (Fig. 2b) consists of a central lamella of aegirine-jadeite (pale tan, $Z \wedge a = 4°$) bordered by zones of jadeite (pleochroic pink to purple, $Z \wedge c = 54°$). Contacts between the two types cut across the cleavage in the acmitic core, and follow grain boundaries. Some jadeite rims show a pronounced optical zoning, apparently related to increasing Mn content.

In SM89 (Fig. 1a) euhedral to subhedral crystals (1–2 mm) of aegirine-jadeite (colorless, $Z \wedge a = 3–4°$) occur in an albite + quartz matrix. Pale violet pyroxene (impure jadeite) forms overgrowths on these cores (Fig. 2a), penetrating along cleavages and forming irregular replacements along other fractures. The jadeite commonly divides originally

euhedral pale cpx into a series of "islands". The contacts are in detail very irregular, showing that the violan has formed by replacement of the aegirine-augite, rather than simultaneous growth of exsolution.

Similar relationships are visible in SM7 and SM102 (Fig. 1c, 1d) , but here the pale aegirine-jadeite crystals ($Z \wedge a$ = 7–9°) are packed with tiny (1–5 μm) euhedra of braunite and hematite. Pale violet ($Z \wedge a$ = 58–60°) chloromelanite, without opaque inclusions, forms rims, veins and replacement patches on and in the aegirine-jadeite grains (Fig. 2c, d). The contacts commonly appear smooth and "rational" at low magnification, but are irregular in detail. In SM7 (Fig. 1d) dark violet omphacite locally forms a distinct outer rim on either the pale chloromelanite or directly on aegirine-jadeite cores. This dark omphacite is also seen as individual grains, commonly aligned in trains within granular masses of aegirine-augite or in protoclastic zones around such masses. The texture/composition relations in these samples thus suggest that the various jadeitic or omphacitic pyroxenes have grown later than, and replaced, "primary" pyroxenes of aegirine-jadeite composition.

(3) Veins of tan to dark reddish brown "schefferite" (manganoan Di–Ac series) occur several places in the ore body and the hanging wall. Two general types are recognized: (a) coarsely euhedral tan to reddish pyroxene prisms 1–2 cm long in a matrix of albite + quartz and commonly coarse dark red piemontite (SM86, SM102, To-A; see appendix); (b) veins of fine-grained, massive light brown pyroxene fels with patches of albite. The latter veins show a hornfels-like texture, and the pyroxene grains are choked with inclusions of albite and braunite. The textures suggest recrystallization of an original coarse-grained pyroxene to a mosaic, but without textural equilibration.

(4) Nearly all specimens containing chloromelanitic or omphacitic pyroxenes show some degree of secondary breakdown of the sodic pyroxene to clinopyroxene + albite + quartz symplectites, similar to those produced in eclogites by postmetamorphic uplift. In some cases this breakdown has resulted in rather coarse symplectites (grain size 1–10 μm). Sample SM101 is an albite pyroxenite with textures suggesting that it is an extreme example of the process. In sample SM50, such symplectites are overgrown by clinopyroxene porphyroblasts, indicating that this coarse symplectitization occurred relatively early in the retrograde history. A very fine-grained symplectite, nearly unresolvable under the microscope, is a ubiquitous retrograde metamorphic product.

Analytical results

Nearly all of the pyroxenes analyzed in this study are chemically heterogeneous, even within optically homogeneous areas; this is a common feature of blueschist-facies clinopyroxenes (Essene and Fyfe, 1967; Carpenter, 1980). In addition, many samples contain two or more distinct generations of pyroxene, as described above. Average analyses for each sample, or for recognizable groupings within each sample, are given in Table 2 and Figure 3. Figure 4 shows the individual data points for all samples, and gives an idea of the significance of the averages given in Table 2.

Calculation of formulae and end members

The analyses presented here have been screened to reject those with analytical sums outside the 98.5-101.5% range, or with $Si^{IV} > 2.02$ (Cameron and Papike, 1981). The oxidation state of Fe was calculated assuming charge balance over 4 cations (M^{3+} = Na + Al^{IV}-Al^{VI}-2Ti). Where Si^{IV} was > 2.00, it was adjusted to this value and the remaining cations renormalized to 2.00, thus assuming full M1 + M2 occupancy. At St. Marcel, the nearly ubiquitous presence of braunite, and the common presence of hematite, suggest that all Fe should be present as Fe^{3+}. This agrees with the calculations; a few of the pyroxenes contain trivial amounts of Fe^{2+}, whereas most contain none (Table 1). For those pyroxenes which still have a charge deficiency after conversion of Fe^{2+} to Fe^{3+}, Mn^{2+} was oxidized to Mn^{3+}, producing the manganacmite molecule (Penfield, 1893; Mottana *et al.*, 1979).

On the assumption of full site occupancy, the end members were then calculated in the order $CaTiAl_2O_6$ (titan-Tschermak's molecule), $CaAl_2SiO_6$ (Tschermak's molecule), $NaMn^{3+}Si_2O_6$ (manganacmite), $NaFe^{3+}Si_2O_6$ (acmite), $NaAlSi_2O_6$ (jadeite), $CaMnSi_2O_6$ (johannsenite), $CaFeSi_2O_6$ (hedenbergite), $CaMgSi_2O_6$ (diopside), $Mg_2Si_2O_6$ (enstatite), $Ca_2Si_2O_6$ (wollastonite). This procedure gives the maximum possible contents of acmite and manganacmite, and allows all errors in balance between 1^+ and 3^+ cations to affect the jadeite content. It also gives maximum contents of johannsenite and hedenbergite by ignoring possible components such as ferrosilite ($Fe_2Si_2O_6$) and kanoite ($MnMgSi_2O_6$), and lets all imbalance between 2^+ cations in M1 and

Table 2. Averaged analyses of clinopyroxenes

Sample No.	SM 4	SM 7	SM 7	SM 7	SM 7	SM 36	SM 50	SM 51	SM 51	SM 51
No.anal.	(10)	(7)	(15)	(5)	(2)	(10)	(6)	(2)	(2)	(2)
Type	Vein	Core	Pale Viol	Dark Viol	Sec	Pale Viol	Sec	Pale Viol	Pale Viol	Sec
SiO_2	54.64	56.00	56.20	56.21	53.43	54.52	54.76	55.61	55.77	53.96
TiO_2	0.0	0.14	0.07	0.14	0.08	0.0	0.10	0.21	0.26	0.10
Al_2O_3	1.05	11.92	12.80	11.27	0.58	5.30	1.62	8.48	9.65	2.63
Fe_2O_3	6.33	15.20	8.06	1.80	13.18	11.61	5.23	11.07	4.89	15.47
FeO	0.0	0.0	1.55	0.0	0.0	0.0	0.0	1.06	0.80	0.0
MnO^t	0.59	0.45	1.20	1.73	0.83	0.79	0.87	0.60	1.53	0.82
MgO	14.09	1.88	3.76	8.12	10.33	8.18	14.01	6.28	7.93	8.34
CaO	20.34	2.54	5.19	11.57	14.55	11.69	19.17	8.53	10.74	12.05
Na_2O	3.16	13.07	11.03	8.03	6.13	7.59	3.47	9.25	7.91	7.27
	100.20	101.20	99.87	98.87	99.11	99.68	99.23	101.10	99.48	100.64
Formula proportions (on a total positive charge of 4)										
Si	1.986	1.985	2.002	1.999	1.985	1.990	1.999	1.987	1.998	1.982
Al^{IV}	0.014	0.015	-	0.001	0.015	0.010	0.001	0.013	0.002	0.018
Z	2.000	2.000	(2.00)	2.000	2.000	2.000	2.000	2.000	2.000	2.000
Al^{VI}	0.031	0.483	0.538	0.471	0.010	0.218	0.069	0.344	0.406	0.096
Ti	-	0.004	0.002	0.004	0.002	-	0.003	0.006	0.007	0.003
Fe^{3+}	0.173	0.406	0.225	0.048	0.368	0.319	0.144	0.298	0.132	0.428
Fe^{2+}	-	-	0.035	-	-	-	-	0.032	0.024	-
Mn^{3+}	0.018	0.014	-	0.030	0.026	0.010	0.027	-	-	0.010
Mn^{2+}	-	-	0.036	0.022	-	0.014	-	0.018	0.046	0.016
Mg	0.763	0.099	0.200	0.430	0.572	0.445	0.762	0.335	0.423	0.457
Ca	0.792	0.096	0.198	0.441	0.579	0.457	0.750	0.327	0.412	0.474
Na	0.223	0.898	0.763	0.554	0.442	0.537	0.246	0.641	0.549	0.518
Charge	11.99	11.99	12.00	12.00	11.96	12.00	12.00	12.00	12.00	12.00
Calculated end-members										
TiTs	-	0.4	-	0.1	0.2	-	-	0.6	0.1	0.3
CaTs	1.4	0.7	-	-	1.0	1.0	-	0.1	-	1.3
Jd	1.6	47.6	53.8	47.1	-	20.8	6.9	34.3	40.7	8.0
Ac	17.3	40.6	22.5	4.8	36.9	31.9	14.4	29.8	13.2	42.8
MnAc	1.8	1.4	-	3.0	2.6	1.0	2.7	-	-	1.0
Joh	-	-	3.6	2.2	-	1.4	-	1.8	4.7	1.6
Hd	-	-	3.5	-	-	-	-	3.2	2.4	-
Di	76.4	8.5	12.7	41.8	56.7	43.3	74.9	27.0	34.0	44.0
Wo	0.8	-	-	-	-	-	-	-	-	-
En	-	0.7	3.7	0.6	0.3	0.6	0.7	3.2	4.2	0.4

M2 sites affect Ca and Mg components. Thus the wollastonite or enstatite residual becomes another measure of the analytical quality.

Manganacmite substitution

The existence of the manganacmite substitution in clinopyroxene was proposed by Penfield (1893) on the basis of his analyses of St. Marcel violan; he determined a $Mn^{3+}/(Mn^{3+} + Mn^{2+}) = 0.70$. This suggestion was generally neglected until revived by Bondi *et al.* (1978) and Mottana *et al.* (1979). They offered two reasons for considering this substitution: the covariance of Na with Mn in the diopside-omphacite pyroxenes (*e.g.* SM103, Fig. 5) and the possibility of explaining the violet color by electron transfer between Mn^{2+} and Mn^{3+} (*cf.* Mottana and Griffin, 1979). To these reasons we can add the high oxidation state of the deposit as demonstrated by Brown *et al.* (1978) and by the mineralogy of the samples described here. Finally, K. Langer (per-

Table 2. (continued)

Samp.	SM	SM	SM	SM	SM	SM	SM	SM	SM	SM
No.	52	52	55	55	72	83	86	87	87	87
No.anal.	(6)	(3)	(2)	(7)	(4)	(7)	(3)	(4)	(5)	(2)
Type	Viol	Sec	Dark Viol	Pale Core	Pale Viol	Viol	Vein	Pale Core	Rims	Sec
SiO_2	55.96	53.91	52.83	55.47	55.00	56.50	53.33	55.19	55.83	55.95
TiO_2	0.0	0.0	0.10	0.0	0.07	0.0	0.0	0.05	0.19	0.19
Al_2O_3	9.76	1.17	1.25	55.47	1.22	11.67	1.23	7.76	9.87	6.71
Fe_2O_3	5.02	11.80	19.03	17.80	4.90	2.02	13.73	13.41	4.87	6.05
FeO	0.81	0.0	0.0	0.0	0.0	0.0	0.0	0.72	0.96	0.50
MnO^t	1.61	0.97	2.30	0.25	0.41	0.79	2.32	0.62	0.71	0.67
MgO	7.89	10.96	6.03	1.24	14.73	8.69	9.59	4.70	7.64	9.90
CaO	10.65	15.51	8.64	1.58	21.31	12.03	14.34	6.57	10.48	13.63
Na_2O	7.93	5.45	9.22	13.43	2.67	8.02	5.93	10.33	8.24	6.64
	99.62	99.77	99.40	100.67	100.31	99.72	100.47	99.34	98.79	100.24
Formula proportions (on a total positive charge of 4)										
Si	2.002	1.987	1.979	1.990	1.991	1.985	1.971	2.013	2.007	2.002
Al^{IV}	-	0.013	0.021	0.010	0.009	0.015	0.029	-	-	-
Z	(2.00)	2.000	2.000	2.000	2.000	2.000	2.000	(2.00)	(2.00)	(2.00)
Al^{VI}	0.411	0.038	0.034	0.451	0.043	0.469	0.025	0.336	0.419	0.283
Ti	-	0.000	0.003	-	0.002	-	-	0.001	0.005	0.005
Fe^{3+}	0.139	0.327	0.536	0.481	0.134	0.053	0.382	0.370	0.161	0.178
Fe^{2+}	0.020	-	-	-	-	-	-	0.012	-	-
Mn^{3+}	-	0.030	0.073	0.008	0.013	0.024	0.050	0.008	0.006	-
Mn^{2+}	0.049	-	-	-	-	-	0.023	0.019	0.016	0.020
Mg	0.421	0.602	0.337	0.066	0.795	0.455	0.528	0.258	0.410	0.529
Ca	0.408	0.613	0.347	0.061	0.827	0.453	0.568	0.259	0.405	0.524
Na	0.550	0.390	0.670	0.934	0.187	0.546	0.425	0.736	0.576	0.461
Carghe	12.00	11.99	11.96	12.00	11.99	11.98	12.00	12.00	12.00	12.00
Calculated end-members										
TiTs	-	-	0.3	-	0.2	-	-	-	-	-
CaTs	-	1.3	1.5	1.0	0.5	1.5	2.5	-	-	-
Jd	41.1	2.5	1.9	44.1	3.8	45.4	-	33.6	41.9	28.3
Ac	13.9	32.7	53.7	48.1	13.4	5.3	38.2	37.0	16.1	17.8
MnAc	-	3.0	7.3	0.8	1.3	2.4	5.0	1.2	0.6	-
Joh	2.5	-	-	-	-	-	2.3	2.7	1.6	2.0
Hd	2.0	-	-	-	-	-	-	1.2	-	-
Di	32.9	60.0	32.9	5.1	79.5	43.8	52.0	22.2	38.9	50.9
Wo	-	-	0.4	-	1.3	-	-	-	-	-
En	4.1	0.1	-	0.8	-	0.9	0.4	1.9	1.1	1.0

sonal communication) has found evidence for the presence of Mn^{3+} in these pyroxenes by optical absorption studies in the visible region.

Our calculated structural formulae (Table 1) show that in over half of the pyroxenes, all Mn is present as Mn^{3+}, leaving a small charge imbalance (always <0.02). About one-fourth show both Mn^{2+} and Mn^{3+} and are thus charge-balanced, whereas the remainder show only Mn^{2+}. The total amounts of (MnAc+Joh) in the averaged analyses are on the order of 1–4%, so that they lie essentially within the error margin induced by analytical uncertainty in the analysis. Our analyses thus suggest that manganacmite substitution is important in these pyroxenes, but cannot give precise values for Mn^{2+}/Mn^{3+}. However, it is probably significant that many of the darkest violans, with MnO^T contents over 2%, appear to contain both Mn species. The maximum values observed are in the omphacites of SM 103, with some individual analysis

Table 2. (continued)

Sample	SM	SM	SM	SM	SM	SM	SM	SM	SM
No.	88	88	89	89	90	94	94	100	100
No.anal.	(3)	(8)	(5)	(7)	(6)	(5)	(4)	(6)	(5)
Type	Pale Core	Viol Rims	Pale Core	Viol Rims	Viol	Blade Viol	Gran Viol	Tan Cpx	Viol
SiO_2	53.98	56.47	54.76	57.23	55.90	55.86	55.28	53.13	54.08
TiO_2	0.10	0.0	0.0	0.0	0.0	0.04	0.08	0.08	0.07
Al_2O_3	11.26	17.27	11.86	18.75	10.40	9.17	9.05	0.94	0.84
Fe_2O_3	16.94	7.13	17.51	5.70	0.97	6.61	11.49	14.55	13.27
FeO	0.0	0.0	0.0	0.0	0.0	0.88	1.49	0.0	0.0
MnO^t	0.16	0.97	0.26	0.66	1.12	1.21	0.43	0.44	1.09
MgO	1.15	1.88	0.93	1.93	9.86	7.30	4.46	10.00	10.12
CaO	1.62	2.68	1.27	2.58	14.00	9.89	6.45	14.64	14.50
Na_2O	13.43	13.17	13.68	13.44	6.96	8.42	10.36	5.88	6.25
	98.64	99.57	100.27	100.29	99.21	99.38	99.09	99.66	100.22
Formula proportions (on a total positive charge of 4)									
Si	1.968	1.978	1.966	1.976	1.978	2.009	2.012	1.975	1.989
Al^{IV}	0.032	0.022	0.034	0.024	0.022	-	-	0.025	0.011
Z	2.000	2.000	2.000	2.000	2.000	(2.00)	(2.00)	2.000	2.000
Al^{VI}	0.452	0.690	0.468	0.738	0.412	0.390	0.390	0.016	0.025
Ti	0.003	-	-	-	-	0.001	0.002	0.002	0.002
Fe^{3+}	0.465	0.188	0.473	0.148	0.026	0.198	0.341	0.407	0.367
Fe^{2+}	-	-	-	-	-	0.009	0.021	-	-
Mn^{3+}	0.005	0.029	0.025	0.019	0.034	-	-	0.014	0.034
Mn^{2+}	-	-	-	-	-	0.037	0.013	-	-
Mg	0.063	0.098	0.050	0.099	0.520	0.393	0.243	0.554	0.555
Ca	0.063	0.101	0.049	0.095	0.531	0.383	0.253	0.583	0.571
Na	0.949	0.894	0.952	0.900	0.478	0.590	0.735	0.424	0.446
Charge	11.95	11.99	11.98	11.98	11.98	12.00	12.00	12.00	12.00
Calculated end-members									
TiTs	0.3	-	-	-	-	-	-	0.2	0.2
CaTs	2.6	2.2	3.4	2.4	2.2	-	-	1.6	0.7
Jd	42.6	66.8	43.4	71.4	39.0	39.0	39.0	-	1.8
Ac	46.8	18.8	47.3	14.8	.6	19.8	34.1	40.7	36.7
MnAc	0.5	2.9	2.5	1.9	3.4	-	-	1.4	3.4
Joh	-	-	-	-	-	3.7	1.3	-	-
Hd	-	-	-	-	-	0.9	2.1	-	-
Di	3.4	7.9	1.5	7.1	50.9	33.7	21.9	55.4	55.5
Wo	-	-	-	-	-	-	-	0.3	-
En	1.4	0.8	1.7	1.4	0.6	2.8	1.3	-	0.4

points giving 4–4.5% MnO^T and up to 13% Mn–Ac (Fig. 5).

Di–Jd–Ac variations

The analyzed pyroxenes never contain over 6% of components other than Di, Jd, Ac and MnAc. The individual analyses are therefore presented in Figures 3, 4, 7 in terms of end members Jd, Ac + MnAc, and "other" (augite).

The compositional variations within some samples are very large (Figures 3, 4), so that each of the textural types discussed above covers large areas of the Di–Ac–Jd compositional plane. In general, the diopside and omphacite compositions are associated with the bladed or lamellar "violans". Aegirine-jadeite and chloromelanite pyroxenes are mostly found in massive pyroxene-rich samples. Di–Ac pyroxenes are usually either secondary after omphacites and chloromelanites, or occur in late, coarse-grained veins.

Table 2. (continued)

Sample	SM	SM	SM	SM	SM	SM	VM	VM
No.	101	102	102	103	103	103	1	7
No.anal.	(12)	(10)	(17)	(7)	(10)	(8)	(10)	(5)
Type	Viol	Pale Core	Viol Rims	Diop	Pale Viol	Dark Viol	Dark Viol	Dark Viol
SiO_2	54.98	54.41	55.51	54.73	55.40	55.51	55.67	56.35
TiO_2	0.07	0.09	0.09	0.09	0.21	0.16	0.10	0.0
Al_2O_3	6.21	9.77	10.23	0.80	3.52	7.74	7.32	9.56
Fe_2O_3	8.78	18.34	9.21	0.23	0.47	2.32	0.71	3.43
FeO	0.0	0.0	0.0	0.0	0.0	0.0	0.0	0.0
MnO^t	0.54	0.27	0.96	0.54	1.90	3.38	1.19	0.86
MgO	9.02	1.65	5.21	16.99	14.36	9.57	12.70	9.71
CaO	12.86	2.33	8.50	24.30	20.43	13.76	17.04	12.74
Na_2O	7.30	13.10	9.80	0.97	3.08	6.99	5.09	7.65
	99.76	99.96	99.51	99.13*	99.37	99.43	99.82	100.30
Formula proportions (on a total positive charge of 4)								
Si	1.985	1.972	1.996	1.997	1.998	1.984	1.971	1.979
Al^{IV}	0.015	0.028	0.004	0.003	0.002	0.016	0.029	0.021
Z	2.000	2.000	2.000	2.000	2.000	2.000	2.000	2.000
Al^{VI}	0.249	0.389	0.429	0.032	0.147	0.310	0.277	0.375
Ti	0.002	0.002	0.002	0.002	0.006	0.004	0.003	-
Fe^{3+}	0.239	0.500	0.249	0.006	0.013	0.062	0.019	0.091
Fe^{2+}	-	-	-	-	-	-	-	-
Mn^{3+}	0.017	0.008	0.005	0.017	0.050	0.102	0.036	0.026
Mn^{2+}	-	-	0.020	-	0.008	-	-	-
Mg	0.485	0.089	0.279	0.924	0.772	0.510	0.670	0.508
Ca	0.497	0.090	0.327	0.950	0.789	0.527	0.646	0.479
Na	0.511	0.920	0.683	0.069	0.215	0.484	0.349	0.521
Charge	11.99	11.96	12.00	11.99	12.00	11.98	11.96	11.95
Calculated end-members								
TiTs	0.2	0.3	0.2	0.2	0.2	0.4	0.3	-
CaTs	1.1	2.3	-	-	-	1.2	2.3	2.1
Jd	23.8	36.6	42.9	3.0	14.7	29.8	25.4	35.4
Ac	23.9	50.0	24.9	0.6	1.3	6.2	1.9	9.1
MnAc	1.7	0.8	0.5	1.7	5.0	10.2	3.6	2.6
Joh	-	-	2.4	-	0.8	-	-	-
Hd	-	-	-	-	-	-	-	-
Di	48.4	6.4	27.9	92.4	77.2	51.0	62.0	45.8
Wo	-	-	1.2	-	0.4	0.3	-	-
En	0.1	1.3	-	1.2	-	-	2.5	2.5

* Includes 0.48% SrO (range 0.0-1.4%)

Several samples (SM7, 55, 88, 89, 102; VM116, 117) contain aegirine-jadeite pyroxenes of a composition previously believed to be "forbidden" (Coleman and Clark, 1968), but documented by Essene and Fyfe (1967) in Franciscan blueschists and by Carpenter (1979) from Turkish blueschist-facies rocks. Many of these (SM88, 89; VM116, 117) contain a second pyroxene of impure jadeite composition. Textures described above (Fig. 1) leave little doubt that the jadeitic pyroxenes replace the aegirine-jadeites. Furthermore, the "primary" pyroxenes of VM116 and 117 lie in the "gap" of SM88 and 89, and the spread of analysis points closes any possible "gap" (Fig. 4). Hence these samples cannot be used to infer the presence of a solvus along the Jd-Ac join. Samples SM7 and SM102 (Fig. 7) show zoning and replacement of aegirine-augite by chloromelanite. The spread of all the analyses al-

Table 2. (continued)

Sample	VM	VM	VM	VM	VM	VM
No.	104	104	116	116	117	117
No.anal.	(6)	(2)	(6)	(6)	(9)	(5)
Type	Viol	Sec	Pale Core	Viol Rims	Pale Core	Viol Rims
SiO_2	56.71	54.79	55.76	57.12	56.13	57.28
TiO_2	0.10	0.0	0.13	0.08	0.15	0.05
Al_2O_3	9.92	1.07	12.95	16.15	14.50	18.19
Fe_2O_3	0.94	0.96	14.70	8.01	13.87	8.69
FeO	0.0	0.0	0.0	0.0	0.0	0.0
MnO	1.35	1.04	0.38	1.28	0.16	0.15
MgO	10.00	16.33	1.39	2.10	0.68	0.70
CaO	14.22	23.59	1.64	3.02	0.90	0.82
Na_2O	6.79	1.31	13.67	13.01	14.11	14.40
	100.03	99.09	100.62	100.77	100.50	100.28
Formula proportions (on a total positive charge of 4)						
Si	1.996	1.996	1.977	1.988	1.983	1.988
Al^{IV}	0.004	0.004	0.023	0.012	0.017	0.012
Z	2.000	2.000	2.000	2.000	2.000	2.000
Al^{VI}	0.408	0.042	0.518	0.651	0.586	0.732
Ti	0.003	-	0.003	0.002	0.004	0.001
Fe^{3+}	0.025	0.026	0.392	0.210	0.369	0.227
Fe^{2+}	-	-	-	-	-	-
Mn^{3+}	0.030	0.030	0.011	0.030	0.005	0.004
Mn^{2+}	0.010	0.002	-	0.008	-	-
Mg	0.525	0.887	0.073	0.109	0.036	0.036
Ca	0.536	0.921	0.062	0.113	0.034	0.030
Na	0.463	0.093	0.940	0.878	0.966	0.969
Charge	12.00	12.00	11.96	12.00	11.99	11.99
Calculated end-members						
TiTs	0.2	-	0.4	0.2	0.4	0.1
CaTs	-	0.4	1.7	0.8	0.9	1.0
Jd	40.8	3.8	50.1	63.8	57.7	72.2
Ac	2.5	2.6	39.2	21.0	36.9	22.7
MnAc	3.0	3.0	1.1	3.0	0.5	0.4
Joh	1.0	0.2	-	0.8	-	-
Hd	-	-	-	-	-	-
Di	52.2	88.7	4.2	9.5	2.1	1.9
Wo	-	1.4	-	-	-	-
En	0.3	-	1.5	0.7	0.8	0.9

lows the possibility of a real compositional gap (Fig. 4) but the textural relations again suggest that inference of a solvus from these data would be premature.

Apparently primary chloromelanites with compositions similar to one of Penfield's (1893) analyses (D in Fig. 3) are common. These are often zoned to, or appear to coexist with, omphacites with relatively high (Ac + MnAc) contents. However, the range of all point analyses in this area of the figure strongly argues for a continuous variation in chemical composition between chloromelanites (up to Ac_{45}) and omphacites with Ac $\simeq$ 0.

Diopsides with Jd + Ac < 20% make up a large proportion of the previously analyzed samples (Fig. 3), but are rare in our material. Earlier analyses showed a large compositional gap between these diopsides and the omphacites, and this was supported by microprobe data on individual samples (Mottana *et al*, 1977, 1979; Brown *et al.*, 1978). Two of our samples, however, lie within this gap. SM103, described above, shows continuous zoning from diopside to omphacite, as well as replacement of less sodic pyroxenes by omphacite (Figs. 4, 7). Mottana *et al.* (1979) gave anlayses of the core ($Jd_{42}Ac_2$) and rim ($Jd_{45}Ac_9$) of a euhedral omphacite from a vug. Our section VM1 cuts through the wall of this vug; our point analyses extend the compositional range in this sample to $Jd_{16}Ac_6$ (Fig. 4). There seems to be no evidence in our material for a solvus between diopside and omphacite at the peak of metamorphism.

The pyroxenes along the Di–Ac join from Ac_{10} to Ac_{50} fall mainly into two groups: late veins, and secondary pyroxenes. Where the secondary pyroxene can be related to a primary one, it is obvious that the breakdown has resulted from loss of the Jd component to form the albite now seen in symplectites. In the case of SM72 the albite forms collars of euhedral blocky grains around mosaics of pyroxene, in a quartz matrix. The texture suggests breakdown of euhedral omphacite grains to clinopyroxene + albite.

X-ray results

The unit-cell parameters and lattice types of St. Marcel pyroxenes are listed in Table 3 and plotted

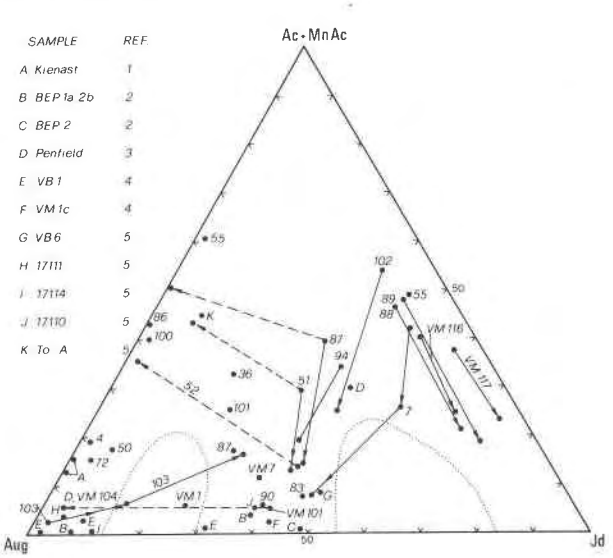

Fig. 3. Averaged analyses of St. Marcel clinopyroxenes (Table 1). Arrows show age sequences deduced from textural relations. Dashed lines connect primary and secondary (acmitic) pyroxenes. Dotted lines show possible compositional gaps. References to published data: (1) Kienast (1973); (2) Brown *et al.* (1978); (3) Penfield (1893); (4) Mottana *et al.* (1979); (5) Bondi *et al.* (1978).

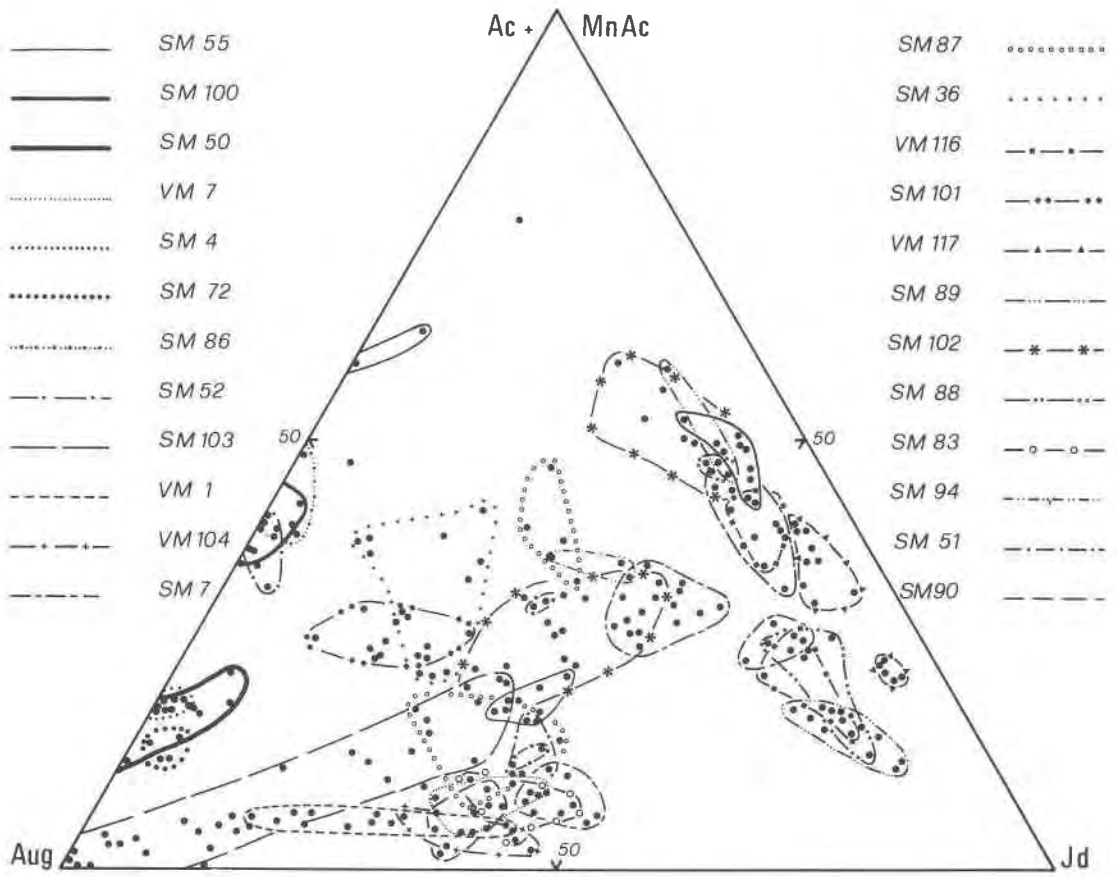

Fig. 4. Individual complete analyses of St. Marcel clinopyroxenes.

in Figure 6. The measured values are uneven in quality, in spite of their low standard errors, because they are affected to different degrees by the inhomogeneity of the samples. An estimate of their accuracy can be deduced from the number of peaks used during the final cycle of refinement (Table 3) in order to reduce the errors within acceptable limits (below 0.010Å). Furthermore, in each sample, data could be obtained only for the most abundant types of pyroxene, except where large color differences made it possible to distinguish among the individual grains under the binocular microscope. However, the data are internally consistent, and consistent with previous determinations of the St. Marcel pyroxenes (Mottana *et al.*, 1977; Bondi *et al.*, 1978; Brown *et al.*, 1978), which are also listed in Table 3.

The consistency of the results shows up not only in the parameter *vs.* parameter plots, but also in the plots of each parameter *vs.* the unit-cell volume (Fig. 6). The volume is considered to be the most reliable indicator of the overall chemical composition of a pyroxene not only because the possible errors in individual cell parameters are cancelled out, but also because it accounts both for the radii of the cations in the M1 and M2 sites and for the charge of the M2 cation (Ribbe and Prunier, 1977).

The *a* and *b* parameters are linearly related to the volume for all the *C*-pyroxenes, because the same parameters for the three end-members involved in these solid solutions also vary linearly (Fig. 6). However, the variations of *c* and β with volume are distinctly non-linear. They are divided into the two linear portions Jd–Ac and Ac–Di. The Ac component controls the unit-cell behavior of the system as a whole, and moves the data away from the Jd–Di tieline. This contrasts with the behavior previously observed for omphacites (Edgar *et al.*, 1969) and is consistent with the presence of solid solutions other than Di–Jd.

Despite the uncertainties due to sample heterogeneity, all the pyroxenes with the primitive lattice appear to follow a trend parallel to the overall one, but slightly displaced, particularly for the *c* and *b* parameters (possibly also for beta, but the errors

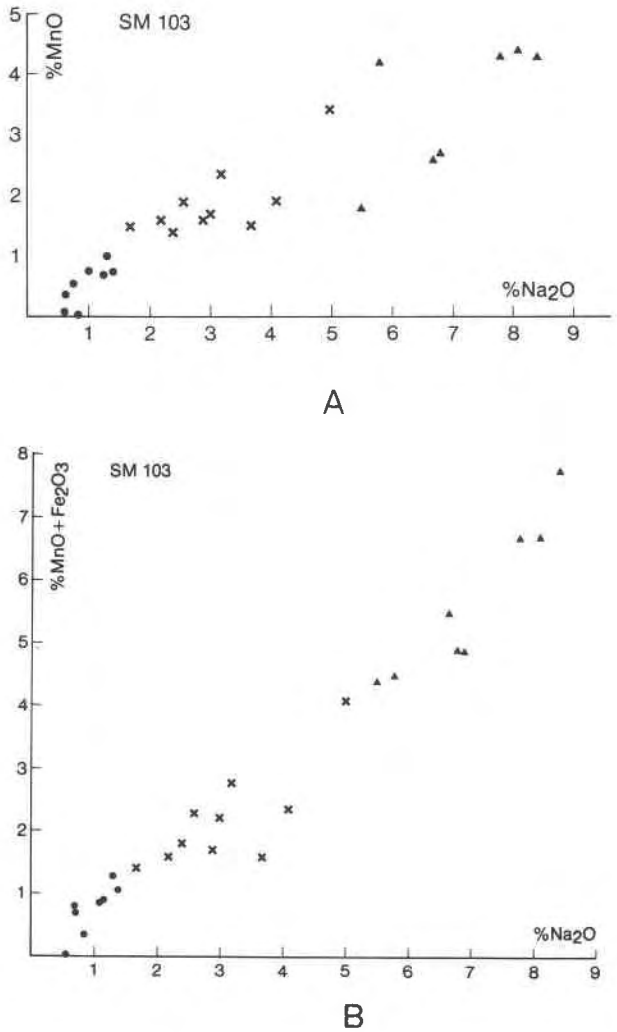

Fig. 5. Correlation between Na + Mn + Fe in zoned grains of SM103, individual analysis points. Dots, pale cores; crosses, pale violan; triangles, dark violan. (a) Na_2O *vs.* MnO^T (wt.%, all Mn as MnO); (b) Na_2O *vs* $MnO^T + Fe_2O_3$ (wt.%).

are large). This implies that the ordering typical of such pyroxenes can also be deduced from their cell parameters, and suggests a short cut to the time-consuming work of determining symmetry by single-crystal methods, particularly where the samples are heterogeneous and need to be analyzed repeatedly. For example, the lattice type of sample SM94 could not be determined satisfactorily due to its irregular mosaic texture. It may belong to the P-lattice type on the basis of its position in Figure 6. This sample is significant in that it is a chloromelanite with a high acmite content and thus confirms the outline of the P field for compositions falling in or near the center of the Di–Jd–Ac triangle (*cf.* Carpenter, 1979).

Discussion

Chemical trends vs. metamorphic history

The metamorphic history of the Zermatt–Saas unit of the Piemonte nappe, as summarized by Dal Piaz and Ernst (1978), involved prograde metamorphism to eclogite-facies conditions, followed by moderate heating and rapid uplift that lead to successive overprints of blueschist- and greenschist-facies assemblages. The mineral assemblages formed during the metamorphic peak generally obliterated any preexisting mineralogy, whereas the latter overprints have only partly removed the evidence for early high-*P*, low-*T* metamorphism.

The St. Marcel rocks show unusually good preservation of these early high-*P* mineral assemblages. The widespread coexistence of omphacite (Jd_{50}) + albite + quartz and jadeite + albite + quartz, and the presence of lawsonite in the footwall rocks, indicate *maximum P, T* conditions of 500°C, 14 kbar, whereas the estimates of 300° ± 50°C, 8 ± 1 kbar by Brown *et al.* (1978) may give *minimum P, T* conditions. Studies of eclogites in nearby areas of the nappe (Ernst and Dal Piaz, 1978; our unpublished data) give *P, T* estimates of 400–500°C, 10-12 kbar. The complicated chemical variations observed in the St. Marcel clinopyroxenes can only be understood in the context of this complex metamorphic history. The textural relations described above demonstrate that several types of "early" pyroxenes were overgrown by, or replaced by, jadeite or omphacitic varieties (Fig. 7). Early aegirine-jadeites are replaced either by impure jadeite (SM88, 89, *etc.*) or by chloromelanite (SM7, 102). Chloromelanites are in turn overgrown by, or replaced by,

Table 3. Unit-cell parameters of St. Marcel pyroxenes

No.	a(Å)	b(Å)	c(Å)	β(°)	V(Å³)	No. of peaks	Type
SM55	9.560(7)	8.702(8)	5.267(3)	107.46(2)	418.0	12	C
SM72	9.723(3)	8.897(2)	5.260(2)	106.10(1)	437.2	13	C
SM83	9.567(5)	8.764(4)	5.252(2)	106.94(1)	421.2	14	P
SM86	9.699(6)	8.865(5)	5.274(2)	106.73(2)	434.3	11	C
SM88	9.497(8)	8.646(8)	5.241(3)	107.26(2)	411.0	10	C
SM89	9.485(8)	8.631(8)	5.238(3)	107.28(2)	409.5	9	C ?
SM90	9.575(5)	8.770(4)	5.254(2)	106.90(1)	422.1	13	P
SM94	9.588(6)	8.768(5)	5.259(3)	106.97(4)	422.9	8	
SM100	9.711(4)	8.855(2)	5.262(2)	105.98(5)	435.0	10	C
Reference data (Bondi et al. 1978; Brown et al. 1978; Mottana et al. 1979)							
17110	9.613(5)	8.785(5)	5.269(3)	106.95(3)	425.6	8	P
17111	9.741(3)	8.922(3)	5.258(2)	105.92(2)	439.4	15	C
17114	9.713(3)	8.894(3)	5.252(2)	106.16(2)	435.8	16	C
VB-6	9.568(4)	8.754(4)	5.265(2)	107.13(2)	421.4	11	P
To-A	9.685(4)	8.852(4)	5.272(2)	106.70(3)	432.9	11	C
VM-1	9.574(6)	8.760(5)	5.252(3)	106.90(3)	421.5	17	P
VB-1	9.716(5)	8.903(5)	5.254(3)	106.01(4)	436.8	15	C
VB-2	9.581(2)	8.770(2)	5.253(1)	106.92(1)	422.3	15	P
BEP-2	9.563(4)	8.755(2)	5.251(2)	106.93(4)	420.6	11	P

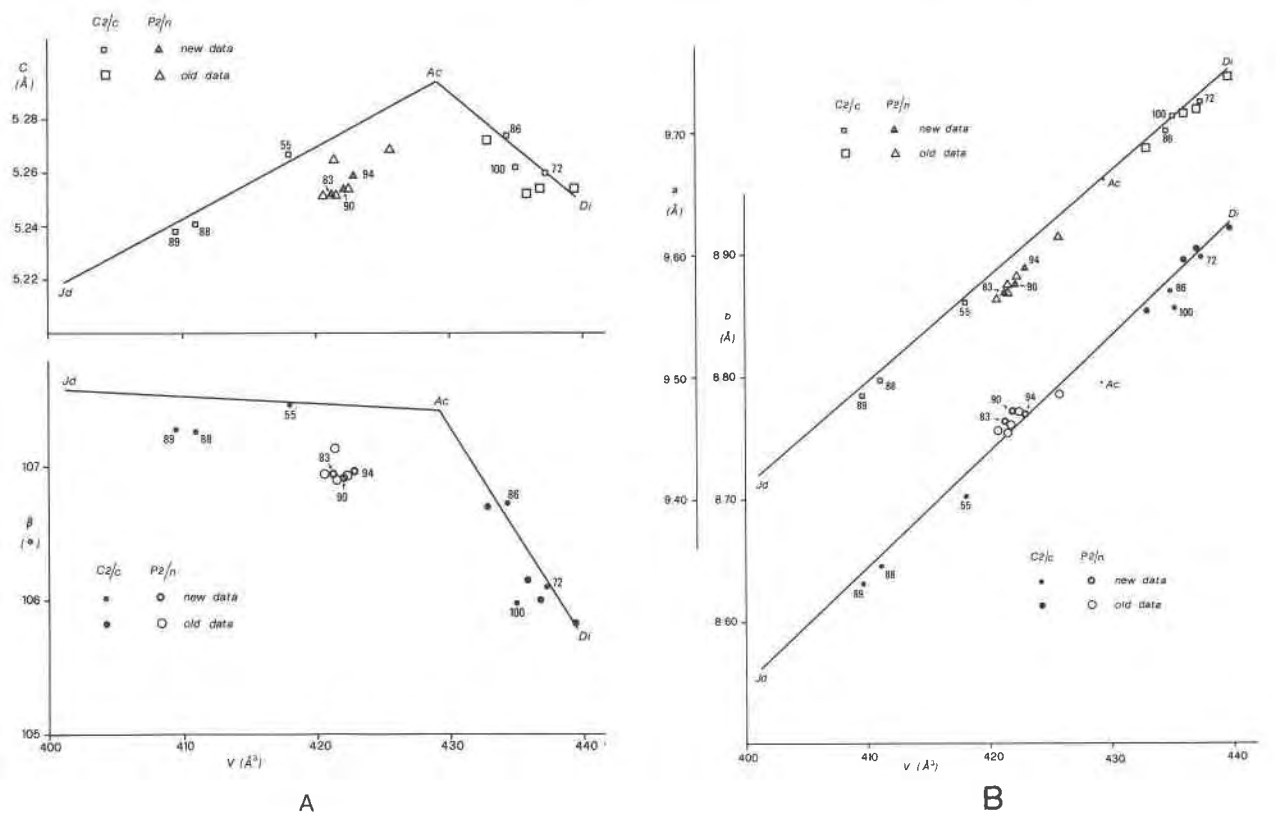

Fig. 6. Correlation of cell parameters for St. Marcel clinopyroxenes (Table 2).

omphacites (SM7, 51, 87). Finally, the diopsides of SM103, which replace tremolite, are overgrown by successively more omphacitic pyroxenes. In all these cases the later generation(s) of pyroxene are richer in Mn.

Two general interpretations of these trends are possible, without being mutually exclusive.

(1) The successive generations reflect prograde metamorphism. The diopsides and aegirine-jadeites may be relatively low-*P*, *T* phases; similar aegirine-jadeites are found, for example, in the lower-grade deposits of the Bernina region (Trommsdorff *et al.*, 1970). The successive development of chloromelanites and diopside-omphacite pyroxene would then reflect the metamorphic breakdown of other phases, freeing Na, Ca, Fe and Mg (and Mn) for reaction with the early pyroxenes. The nature of these metamorphic reactions is not yet clear, but might involve amphiboles and plagioclase.

(2) The successive generations of pyroxene may all have formed near the peak of metamorphism due to metasomatic introduction of Na, A1, (Ca, Fe, Mg)-rich fluids. Such fluid transport could produce real change in bulk composition and might tend to eliminate extreme pyroxene compositions in favor of omphacite/chloromelanite types. This model is especially attractive in the cases of SM103, which apparently originated as a tremolite + quartz (± diopside) rock, and SM88, an apparently massive pyroxenite. It is also clear from field evidence alone that a fluid phase played an important role in the metamorphism at St. Marcel, producing a large variety of coarse-grained, often mineralogically complex, pre-, syn- and postmetamorphic veins and segregations.

Most of the high-*P* pyroxenes and especially the chloromelanite-omphacite group, show some degree of breakdown to aegirine-augite or impure diopside compositions which coexist with albite. The coarse-grained texture of some retrograde products, and the overgrowth of these by porphyroblasts of acmitic diopside (SM50), suggest that the breakdown reflects the rapid uplift and moderate increase in *T* that followed the high-*P* stage. This is tentatively correlated with the blueschist-facies stage that is well represented in the surrounding metabasites.

Coarse-grained veins and segregations of diopsid-

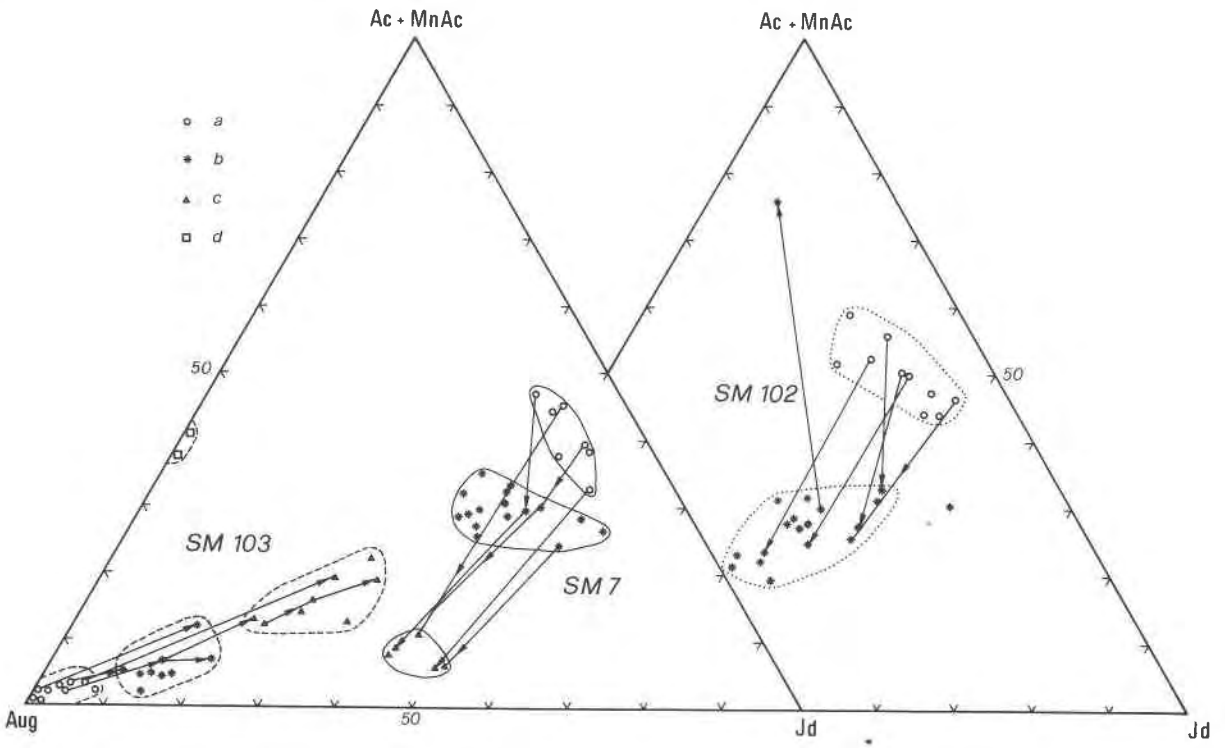

Fig. 7. Point analyses of selected pyroxenes in three samples. Arrows connect zones of individual grains. (a) cores of grains, colorless to grey; (b) "pale violan", pink to light violet; (c) "dark violan", purple-blue color; (d) secondary pyroxenes in SM7.

ic pyroxene + albite ± quartz are abundant in the deposit. Some are obviously late and crosscutting, but the evolutionary position of others is ambiguous because they occur as isolated masses within massive braunite. Experimental work at higher T (Kushiro, 1969) implies that diopside + albite is a low-pressure assemblage. Even if a solvus exists between diopside and omphacite at these low temperatures, the diopside + albite segregations would obviously have a bulk composition that lies on the omphacite side, or at least within the two-pyroxene field, of this solvus. Furthermore, our data suggest that this solvus did not exist at the peak of metamorphism (see below). We therefore conclude that the diopsidic pyroxenes coexisting with albite formed later, and at lower P, than the omphacites.

Compositional gaps

Numerous workers have suggested the existence of compositional "gaps" or "forbidden areas" within the Di–Ac–Jd compositional plane. Dobretsov (1962) and Ginzburg and Sidorenko (1964) proposed a gap between Jd_{60} and Jd_{80} on the Di–Jd join, and extended this to Ac_{50}; the latter authors also proposed a gap from Ac_{20} to Ac_{80} on the Jd–Ac join. Essene and Fyfe (1967) showed that the Jd–Ac gap was filled by pyroxenes from Franciscan blueschists and eclogites. Coleman and Clark (1968) inferred the presence of both gaps, and others (Edgar *et al*, 1969; Onuki and Ernst, 1969; Dobretsov *et al.*, 1971) have argued for the existence of a gap on the Di–Jd join. Recent advances in the subject have come largely from TEM work, combined with microprobe analysis, and are summarized by Carpenter (1979).

The gap on the omphacite–jadeite join, corresponding to a solvus between $C2/c$ and $P2/n$ structures, has been shown to close at higher temperatures (Smith *et al.*, 1980) and at higher acmite contents (Carpenter, 1979, 1980; this work). No coexisting omphacite + jadeite pairs were found in our samples, except perhaps the two distinct rim compositions in SM7 (Fig. 7). However, our data (Fig. 4) also suggest that the omphacite–jadeite gap is present along the Di–Jd join, but narrows and finally closes at Ac contents > 20%. Available X-ray data (Carpenter, 1979, 1980; this work) indicate that the $C2/c$ structural type extends up the Jd–Ac join. This implies that the gap between Ac_{20} and Ac_{80} should not exist, a conclusion that is clearly supported by our analytical data.

A solvus between diopside and omphacite under

low-T conditions was suggested by Brown *et al.* (1978), who found apparently coexisting diopside and omphacite in a St. Marcel specimen, and by Carpenter (1980) from TEM studies. None of our specimens contain *coexisting* omphacite + diopside. VM104 shows decomposition of omphacite to coarse-grained diopside + albite, and SM103 shows zoning of diopside to omphacitic diopside and then to omphacite (Fig. 7). Many of the analyses from samples VM1 and SM103 lie within the "gap" suggested by Brown *et al.* (1978), suggesting that no solvus existed at the peak of metamorphism.

We can suggest two possible explanations of Brown *et al.*'s data. Their two pyroxenes might represent partial breakdown and recrystallization around a solvus at a much lower P (and T?) than is represented by the intermediate pyroxenes analyzed here. Alternatively, they may reflect sequential crystallization, such that the diopside was physically isolated from reaction with Ab at the peak of metamorphism. If the former suggestion is true, then TEM studies of a heterogeneous sample such as VM1 should reveal exsolution on a scale finer than that accessible to the microprobe.

If a solvus does exist between diopside and omphacite at some lower T, than our samples SM36 and SM107 suggest that this solvus also closes at *ca.* Ac_{20}. Both of these pyroxenes coexist with albite ± quartz, and may reflect lower P, T conditions than the more Jd-rich chloromelanites. Carpenter's (1980) proposed phase diagram shows a transition from $P2/n$ omphacites to $C2/c$ chloromelanites without an intervening solvus. This is consistent with our data. Some of our chloromelanites show discontinuous zoning to rims of omphacite, but the complete data set appears to eliminate any possible solvus.

Our data therefore suggest the presence of a limited solvus on the omphacite–jadeite join, extending up to *ca.* Ac_{20}, but argue against the presence of other solvi on this plane at T = 400–500°C, P = 10–12 kbar. Field and petrographic studies make it obvious that the deposit has a complex metamorphic history, and that pyroxenes formed at several stages. Careful textural studies are necessary before the pyroxene compositions in any given sample can be interpreted in terms of phase equilibrium. A better understanding of the pyroxenes may come from detailed studies (now in progress) of their relations to the numerous associated phases, most of which *also* show complex compositional variations. Ultimately, this deposit may allow construction of the phase relations in the Di–Ac–Jd compositional plane at several different temperature-pressure conditions.

Acknowledgments

Microprobe work at Mineralogisk-Geologisk Museum was supported by the Norwegian Research Council for Science and Humanities. Field work was supported by Nansenfondet and the Italian National Research Council, which also supported the X-ray investigations. Thanks are due to Prof. G. Rossi (Pavia) for cooperating in the space-group determinations and to Dr. V. Mattioli (Milan) for donation of many significant specimens. Critical reading by B. B. Jensen and E. J. Essene greatly improved the manuscript.

References

Bearth, P. (1967) Die Ophiolite der Zone von Zermatt-Saas Fee. Beitrage zur Geologischer Karte der Schweiz, N. F., 132.

Bearth, P. (1976) Zur Gliederung der Bündnerschiefer in der Region von Zermatt. Eclogae Geologicae Helvetiae, 69, 149–161.

Bocquet, J., Delaloye, M., Hunziker, J. C., and Krummenacher, D. (1974) K–Ar and Rb–Sr dating of blue amphiboles, micas and associated minerals from the Western Alps. Contributions to Mineralogy and Petrology, 47, 7–26.

Bonatti, E. (1975) Metallogenesis at oceanic spreading centers. Annual Reviews of Earth and Planetary Sciences, Vol. 3, 401–431.

Bonatti, E., Kraemer, T., and Rydell, H. (1972a) Classification and genesis of submarine iron-manganese deposits. In D. Horn, Ed., Ferromanganese Deposits on the Ocean Floor, p. 149–161. International Decade on Ocean Exploration.

Bonatti, E., Fisher, D. E., Joensuu, O., Rydell, H. S. and Beyth, M. (1972b) Iron–manganese–barium deposit from the Afar rift (Ethiopia). Economic Geology, 67, 717–730.

Bonatti, E., Zerbi, M., Kay, R. and Rydell, H. (1976) Metalliferous deposits from the Apennine ophiolites: Mesozoic equivalents of modern deposits from oceanic spreading centers. Geological Society of America Bulletin, 87, 83–94.

Bondi, M., Mottana, A., Kurat, G. and Rossi, G. (1978) Cristallochimica del violano e della schefferite di St. Marcel (Valle d'Aosta). Società Italiana di Mineralogia e Petrologia Rendiconti, 34, 15–25.

Borg, I. Y. and Smith, D. K. (1969) Calculated X-ray powder patterns for silicate minerals. Geological Society of America Memoir, 122.

Boström, K. (1976) The origin and fate of ferromanganoan active ridge sediments. Stockholm Contributions in Geology, 27, 149–243.

Breithaupt, A. (1838) Bestimmung neuer Mineralien. Journal für Praktische Chemie, 15, 320–338.

Brigo, L., Dal Piaz, G. V. and Ferrario, A. (1976) Le mineralizzazioni cuprifere legate ai termini effusivi di alcuni complessi ofiolitici nell'area mediterranea. Bollettino della Associazione Mineraria Subalpina, 13, 352–371.

Brown, P., Essene, E. J. and Peacor, D. R. (1978) The mineral-

ogy and petrology of manganese-rich rocks from St. Marcel, Piedmont, Italy. Contributions to Mineralogy and Petrology, 67, 227–232.

Burckardt, C. E. and Falini, F. (1956) Memoria sui giacimenti italiani di manganese. 20th International Geological Congress Mexico, 5, 221–272.

Cameron, M. and Papike, J. J. (1981) Structural and chemical variations in pyroxenes. American Mineralogist, 66, 1–50.

Carpenter, M. A. (1979) Omphacites from Greece, Turkey, and Guatemala: composition limits of cation ordering. American Mineralogist, 64, 102–108.

Carpenter, M. A. (1980) Mechanism of exsolution in sodic pyroxenes. Contributions to Mineralogy and Petrology, 71, 289–300.

Coleman, R. G. and Clark, J. R. (1968) Pyroxenes in the blueschist facies of California. American Journal of Science, 226, 43–59.

Dal Piaz, G. V. (1971) Alcune considerazioni sulla genesi delle ofioliti piemontesi e dei giacimenti ad esse associati. Bollettino della Associazione Mineraria Subalpina, 8, 365–388.

Dal Piaz, G. V. (1974a) Le métamorphisme alpin de haute pression et basse température dans l'évolution structurale du bassin ophiolitique alpino-apenninique (lère partie: Considerations paléogeographiques). Società Geologica Italiana Bollettino, 93, 437–468.

Dal Piaz, G. V. (1974b) Le métamorphisme de haute pression et basse température dans l'évolution structurale du bassin ophiolitique alpino-apenninique (2e partie). Schweizerische Mineralogische und Petrographische Mitteilungen, 54, 399–424.

Dal Piaz, G. V. and Ernst, W. G. (1978) Areal geology and petrology of eclogites and associated metabasites of the Piemonte ophiolite nappe, Breuil-St. Jacques area, Italian western Alps. Tectonophysics, 51, 99–126.

Debenedetti, A. (1965) Il complesso radiolariti-giacimenti di manganese - giacimenti piritoso-cupriferi - rocce a fuchsite, come rappresentante del Malm nella Formazione dei Calcescisti. Osservazioni nelle Alpi Piemontesi e nella Val d'Aosta. Società Geologica Italiana Bollettino, 84, 131–163.

Delaloye, M. and Desmons, J. (1976) K-Ar radiometric age determinations of white micas from the Piemonte zone, French-Italian western Alps. Contributions to Mineralogy and Petrology, 57, 297–303.

Des Cloizeaux, A. (1862-1874) Manuel de Minéralogie (I, 1862, 66-67; II, 1874, 19–20).

Dobretsov, N. L., (1962) Miscibility limits and mean compositions of jadeite pyroxenes. Akademiya Nauk SSSR Doklady, 146, 676–679.

Dobretsov, N. L., Lavrent'yev, Y. G. and Pospelova, L. N. (1971) Immiscibility in Na–Ca–pyroxenes. Akademiya Nauk SSSR Doklady, 201, 179–182.

Edgar, A. D., Mottana, A. and MacRae, N. D. (1969) The chemistry and cell parameters of omphacites and related pyroxenes. Mineralogical Magazine, 37, 61–74.

Elter, G. I. (1971) Schistes lustrés et ophiolites de la zone piémontaise entre Orco et Doire Baltée (Alpes Graies). Géologie Alpine, 47, 147–169.

Ernst, W. G. and Dal Piaz, G. V. (1978) Mineral parageneses of eclogitic rocks and related mafic schists of the Piemonte ophiolite nappe, Breuil–St. Jacques area, Italian Western Alps. American Mineralogist, 63, 621–640.

Essene, E. J. and Fyfe, W. S. (1967) Omphacite in California metamorphic rocks. Contributions to Mineralogy and Petrology, 15, 1–23.

Evans, H. T., Jr., Appleman, D. E. and Handwerker, D. S. (1963) The least squares refinement of crystal unit cells with powder diffraction data by an automatic computer indexing method (abstract). American Crystallographical Association, Cambridge, Mass., Annual Meeting Program, 42–43.

Franchi, S. (1900) Sopra alcuni giacimenti di rocce giadeitiche nelle Alpi occidentali e nell'Appennino ligure. Bollettino del R. Comitato geologico d'Italia, s.4, 1, 119–158.

Frey, M., Hunziker, J. C., Frank, W., Bocquet, J., Dal Piaz, G. V., Jaeger, E. and Niggli, E. (1974) Alpine metamorphism of the Alps: a review. Schweizerische Mineralogische und Petrographische Mitteilungen, 54, 247–290.

Fry, N. and Fyfe, W. S. (1971) On the significance of the eclogite facies in alpine metamorphism. Geologische Bundesanstalt, Verhandlungen, Wien, 2, 257–265.

Ginzburg, I. V. and Sidorenko, G. A. (1964) Use of X-ray powder patterns to determine some crystal chemical characteristics of the pyroxenes. Mineralogy SSSR Trudy, 15, 81–107.

Huttenlocher, H. F. (1934) Die Erzlaterstättenzonen der Westalpen. Schweizerische Mineralogische und Petrographische Mitteilungen, 14, 22–149.

Jaeger, E. (1973) Die alpine Orogenese im Lichte der radiometrischen Altersbestimmung. Eclogae Geologicae Helvetiae, 66, 205–222.

Kienast, J. R. (1973) Sur l'existence de deux séries différentes au sein de l'ensemble "Schistes lustrés-ophiolites" du Val d'Aosta, quelques arguments fondés sur l'étude des roches métamorphiques. Academie des Sciences, Comptes Rendus Hebdomadaire des Sciences, Serie D, Sciences Naturelles, Paris, 276, 2621–2624.

Kushiro, I. (1969) Clinopyroxene solid solutions formed by reactions between diopside and plagioclase at high pressures. Mineralogical Society of America Special Paper, 2, 179–191.

Mottana, A. and Griffin, W. L. (1979) Pink titanite (greenovite) from St. Marcel, Valle d'Aosta, Italy. Società Italiana di Mineralogia e Petrologia, Rendiconti, 35, 135–143.

Mottana, A., Rossi, G. and Kurat, G. (1977) Riesame del violano. Determinazioni chimiche e strutturali (abstract). Società Italiana di Mineralogia e Petrologia, Rendiconti, 33, 155–156.

Mottana, A., Rossi, G., Kracher, A. and Kurat, G. (1979) Violan revisited: Mn-bearing omphacite and diopside. Tschermaks Mineralogische und Petrographische Mitteilungen, 26, 187–201.

Onuki, H. and Ernst, W. G. (1969) Coexisting sodic amphiboles and sodic pyroxenes from blueschist facies metamorphic rocks. Mineralogical Society of America Special Paper, 2, 241–250.

Pelloux, A. (1922) Miniere e minerali manganesiferi della Valle d'Aosta. Rendiconti dei Lavori dell'Ufficio Invenzioni e Ricerche, Tipografia Senato, Roma.

Penfield, S. L. (1893) On some minerals from the manganese mines of St. Marcel, in Piedmont, Italy. American Journal of Science, 46, 288–295.

Priesshäusser, M. (1909) Die Manganlagerstätte von St. Marcel (Prabornaz) in Piemont. Zeitschrift für praktische Geologie, 17, 396–399.

Ribbe, P. H. and Prunier, A. R., Jr. (1977) Stereochemical systematics of ordered *C2/c* silicate pyroxenes. American Mineralogist, 62, 710–720.

Rondolino, R. (1934) Sopra alcuni minerali di St. Marcel (Valle d'Aosta). Periodico Mineralogia Roma, 5, 123–139.

Rossi, G., Tazzoli, V. and Ungaretti, L. (1978) Crystal-chemical studies on sodic clinopyroxenes. Proceeding 11th Congress I. M. A. Novosibirsk.

Schluttig, E. (1888) Chemisch-mineralogische Untersuchungen von weniger bekannten Silicaten. Zeitschrift für Kristallographie und Mineralogie, 13, 73–76.

Smith, D. C., Mottana, A. and Rossi, G. (1980) Crystal-chemistry of a unique jadeite-rich acmite-poor omphacite from the Nybø eclogite pod, Sørpollen, Nordfjord, Norway. Lithos, 13, 227–236.

Trommsdorff, V., Schwander, H. and Peters, Tj. (1970) Mangansilikate der alpinen Metamorphose in Radiolariten des Julier–Bernina–Gebietes. Schweizerische Mineralogische und Petrographische Mitteilungen, 50, 539–545.

Manuscript received, July 8, 1981;
accepted for publication, November 24, 1981.

Appendix: Sample descriptions

Abbreviations:

Ab, albite; Ap, apatite; Brn, braunite; Cc, calcite; Cpx, clinopyroxene; Hem, hematite; Ksp, K-feldspar; Piem, piemontite; Phl, phlogopite; Phng, phengite (''alurgite''); Qtz, quartz; Rut, Rutile; Sph, sphene (titanite).

SM4: Ab + Cpx vein cutting hanging wall of ore body. Coarse dark reddish brown ''schefferite'' in 1-cm prisms normal to wall of vein, intergrown with Ab. Little or no strain.

SM7: Vein cutting massive Brn of ore body. Assemblage: Qtz + Ab + Ksp + Cpx + Piem + Brn + Sec.Phl. Cpx: pale acmitic cores, violan rims, moderately strained.

SM36: Piem quartzite at upper contact of Brn ore body. Assemblage: Qtz + Ab + Piem + Phng + Cpx + Brn + Hem. Cpx: small scattered grains in Qtz. Moderately strained.

SM50: Vein in brecciated Brn, roof of ore body. Assemblage: Qtz + Ab + Cpx. Cpx: fine-grained Cpx–Ab symplectite overgrown by large crosscutting Cpx porphyroblasts (analyzed). Moderately strained.

SM51: Vein in brecciated Brn, roof of ore body. Assemblage: Qtz + Ab + Cpx + Brn + Sph. Secondary yellow Phl. Cpx: large blades of pale violan, twinned, altered to coarse Cpx + Ab intergrowths. Little or no strain.

SM52: Vein in brecciated Brn, roof of ore body. Assemblage: as SM51. Cpx: large blades of violan, altered to symplectite. Some grains in Qtz surrounded by mosaics of Ab. Little or no strain.

SM55: Coarse-grained mica rich sample from dump. Assemblage: Qtz + Ab + Ksp + Cpx + Phng + Sph. Secondary yellow Phl. Cpx: large strained violan porphyroblasts overgrow foliation and are altered to symplectite rims. Small very dark Di–Ac grains with Brn inclusions.

SM72: Dump sample showing veins in massive Brn. Assemblage in rock: Brn + Piem + Kps + Cc + Qtz. Assemblage in vein: Cpx + Piem + Ab + Ksp + Sph. Cpx: large (6–8 mm) blades of pale pink violan in radial aggregates, slightly strained.

SM83: Dump sample, Brn–Ab–Cpx breccia. Assemblage: Qtz + Ab + Ksp + Cpx + Piem + Brn. Cpx: large strained bladed violans.

SM86: Dump sample. Vein of Cpx in Ab; part of larger vein. Assemblage: Qtz + Ab + Cpx + Sph. Cpx: large crystals of yellow-brown ''johannsenite'', euhedral against Ab, now recrystallized to irregular, bladed mosaic.

SM87: Dump sample. Cpx seam in Piem–Qtz rock. Assemblage: Qtz + Ab + Cpx + Phng + Piem + Brn + Ap + Cc. Cpx: large euhedral grains zoned either to Di–Jd or Di–Ac Di-Ac rims. Little strain.

SM88: Dump sample: Fine-grained violan disseminated in massive Brn, cut by Piem + Ab veinlets. Assemblage: Ab + Cpx + Piem + Brn. Cpx: dark violan (Jd) as lobate rims on clear Cpx (Ac), and as ''veins'' dissecting pale Cpx grains. Little or no strain.

SM89: Dump sample. Fine-grained massive Cpx ''fels'', cut by Qtz veins with disseminated Cpx. Assemblage: Qtz + Ab + Cpx + Phng + Brn. Secondary Piem, kryptomelanite rims on Brn. Cpx: large pale grains (Ac) with rims and veins of violan (Jd). Little or no strain. Moderately strained.

SM90: Dump sample. Coarse-grained dark violan mass. Assemblage: Qtz + Cpx + Ap + Cc. Cpx: large bladed violan grains, some granular, paler violan. Matrix severely strained.

SM94: Dump sample. Coarse, deformed pyroxene vein. Assemblage: Ab + Cpx + Piem + Cc. Sec. yellow Phl. Cpx: large blades of pale Cpx, displaying oscillator zoning, and small granular Cpx (Di).

SM100: Dump sample. Massive light tan pyroxenite (1–3 mm grain size) with pale pink violan bordering irregular, unstrained Ab vein. Violan

shows sieve-porphyroblastic texture, develops euhedrally against Ab vein. Tan Cpx more bladed, fewer inclusions, passes gradually into violan. Metamorphic recrystallization apparently syn- or post-veining. Assemblage: Cpx + Ab + Sph.

SM101: Dump sample: Foliated, strongly strained pyroxenite cut by foliated Piem–Brn–Sph band. Assemblage: Cpx + Piem + Ab + Qtz + Brn + Sph + Rut. Amphibole apparently secondary in euhedral porphyroblasts. Cpx: large bladed crystals, with abundant inclusions of Piem in cores, strongly interdigitated grain boundaries.

SM102: Dump sample. Silicate layer in Brn ore, Assemblage: Ksp (Ba-rich) + Cpx + Phng + Piem (Sr-rich) + Brn. Secondary Phl. Cpx: Granular mass of pale Cpx; grains rimmed or replaced by dark violan. Little strain.

SM103: Min.-Geol. Museum sample. 10 cm-layer of massive tan pyroxenite (1–5 mm grain size) in Brn ore. Assemblage: Cpx + Piem + Qtz. Cpx: large strained prisms of colorless to pale violet Cpx grown across relict tremolite. Strong color zoning to violet along grain margins, cleavages + cracks. Dark violan on grain boundaries, euhedral overgrowths into Qtz, or as separate grains. Darkest violan concentrated next to Brn/Cpx contact.

VM1: Carbonate vug with coarse-grained violan. Assemblage: Cpx + Phl + Cc. Cpx: large, strained bladed grains intergrown with Phl.

VM7: Similar to VM1. Assemblage: Cpx + Ab + Phl + Piem + Brn. Cpx: large prismatic grains, broken into blades and mosaics by intense strain.

VM101: Qtz with thin seam violet amphibole, overgrown by long blades of pale violet Cpx, mostly altered to symplectite. Moderately strained.

VM104: Medium-grained granular rock. Assemblage: Qtz + Ab + Cpx + Phng + Brn. Cpx: large, strained violan grains altered to coarse Di + Ab + Qtz symplectite *and* to finer marginal symplectite.

VM116: Similar to VM104, thin Ab veins. Assemblage: Qtz + Ab + Cpx + Phng + Phl + Sph + Brn + hausmannite. Cpx: pale cores, violan rims (some crosscutting); grains of both type in "equilibrium" contact.

VM117: Large equant, strained Cpx grains in foliated matrix of Ab + Piem + Phl. Cpx: large grains homogeneous and strained. Small grains display strong oscillatory zoning.